Inverse electron demand Diels-Alder pyridazine elimination: synthetic tools for chemical immunology

Geus, M.A.R. de

3

Towards incorporation of *trans*-cyclooctene-modified amino acids in Fmoc solid phase peptide synthesis

T. Hansen and M. S. Kloet contributed to the work described in this Chapter.

3.1 Introduction

The inverse electron demand Diels-Alder (IEDDA) cycloaddition[1] has become an intrinsic component of bioorthogonal chemistry.[2–6] Tetrazine ligation, defined as IEDDA cycloaddition between tetrazines and strained alkenes, is of particular importance when *trans*-cyclooctenes (TCOs)[7,8] acts as dienophiles, as reaction rates within 10^3 – 10^6 $M^{-1}s^{-1}$ are encountered for this reaction pair.[7,9,10] Incorporation of TCO modified lysines via genetic code expansion has proven valuable to enable site-specific protein labeling with fluorogenic tetrazines (Figure 1A).[11–14] The utility of the TCO functionality in this regard is determined by its reaction kinetics, but also by its stability

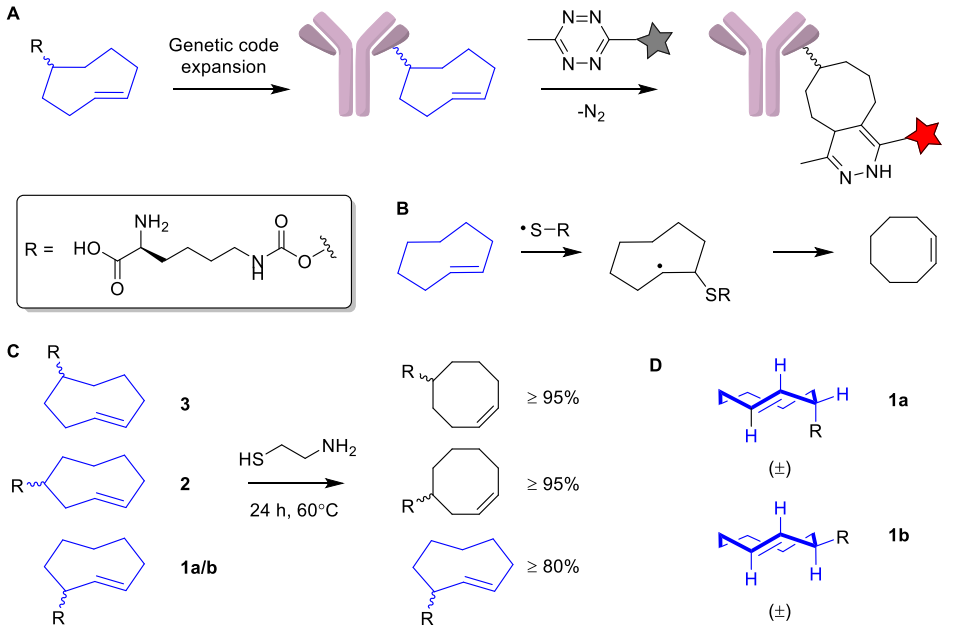

Figure 1 A) Site-specific protein labeling with fluorogenic tetrazines and TCO modified lysines.[2-6] B) Proposed mechanism for thiol-induced TCO isomerization by Fox and co-workers.[17] C) Stability studies on TCO carbamate protected lysines (**1**-**3**) in the presence of cysteamine revealed superior stability for the allylic substituted TCO **1a/b**.[18,19] D) Axial (**1a**) and equatorial (**1b**) isomers of the allylic substituted TCO derivative mentioned in C.

and solubility in biological systems. *In vivo*, high concentrations of thiols[9,10,15] and copper-containing proteins[16] are the primary causes for TCOs to isomerize to their *cis*-cyclooctene counterparts. Fox and co-workers recently demonstrated thiol-induced TCO isomerization to proceed through radical intermediates (Figure 1B).[17] Nikíc *et al*.[18] studied the stability of TCO modified lysines in the presence of cysteamine hydrochloride using ^{1}H-NMR, revealing the allylic TCO carbamate (2-ene, **1a/b**) to possess superior stability compared to 3-ene (**2**) and 4-ene (**3**) isomers (Figure 1C).[18] Within these allylic substituted TCOs, the more reactive axial isomer (**1a**) is also more resistant towards isomerization by cysteamine compared to the equatorial isomer (**1b**, Figure 1D).[19] This finding contradicts general stability trends for TCOs in which increased reactivity towards tetrazines is paired with reduced stability.[9,10]

A recently discovered elimination extension of the tetrazine ligation with TCOs, IEDDA pyridazine elimination,[20] employs allylic substituted TCOs as temporary "cages" to mask the amine functionality of antibody drug conjugates (ADCs),[21,22] protein active sites[23] and immunogenic peptides[24] as TCO carbamates (Figure 2A). Tetrazine ligation is followed by a tautomerization step, leading to liberation of the amine and

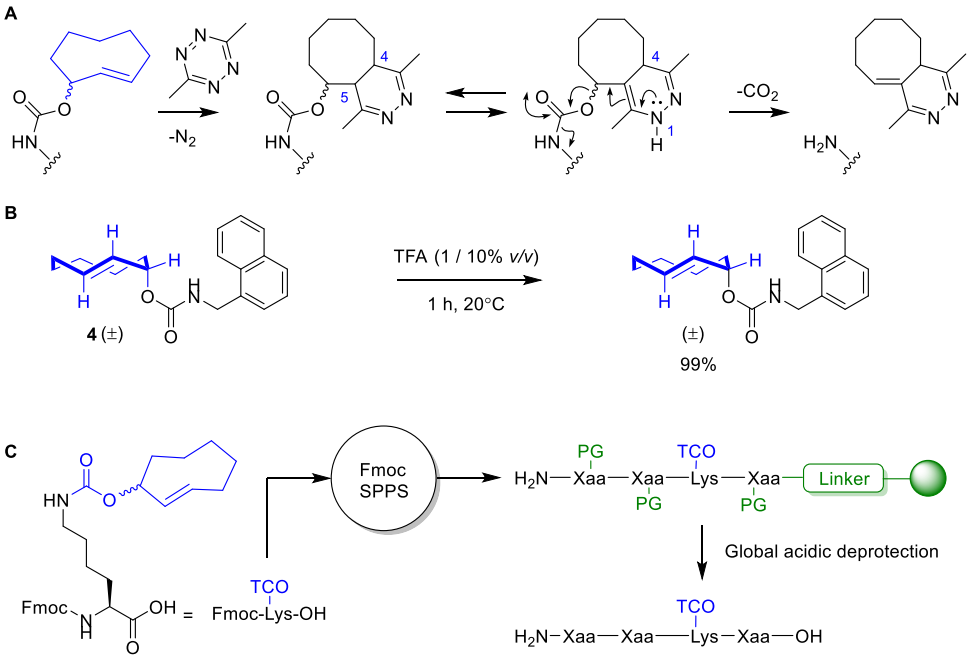

Figure 2 A) Overview of the IEDDA pyridazine elimination reaction.[20] B) Stability data of an allylic substituted TCO carbamate **4** (axial isomer) in the presence of TFA by Robillard and co-workers.[18] C) Synthetic strategy proposed in this Chapter. PG = protecting group; Xaa = unspecified amino acid.

elimination of the pyridazine and CO_2 from a 1,4-dihydropyridazine. Synthesis of these caged biomolecules often hinges on chemoselectivity of amines to obtain the TCO modified carbamate constructs. Solid phase synthetic strategies would omit this necessity and therefore increase the scope of biomolecules available to this decaging method. However, acidic (deprotection) conditions are common to these strategies, and cyclooctenes are reported to react with (strong) acids.[25–27] In this respect, Robillard and co-workers reported full stability for a model axial TCO with allylic carbamate substitution (**4**) in 1% and 10% TFA (*v/v* in $CHCl_3$, 1 hour; Figure 2B).[28] It was hypothesized that the stability of such TCO's[18,19,28] would allow its incorporation in a growing peptide chain during Fmoc solid phase peptide synthesis (SPPS), followed by acidic cleavage of the peptide from the solid support (Figure 2C). This Chapter describes the attempted development of an SPPS-based strategy for TCO-modified peptide synthesis.

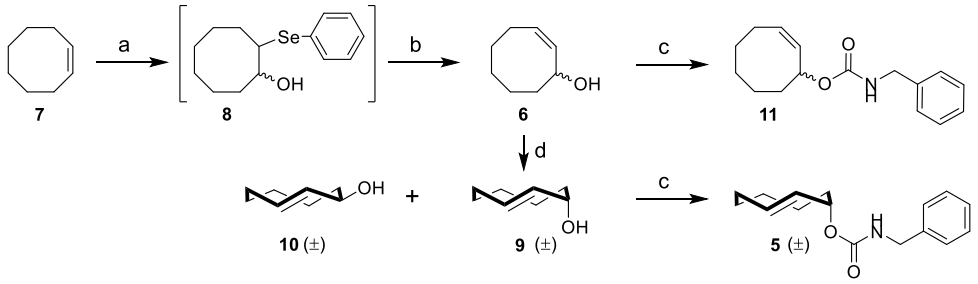

Scheme 1 Synthesis of allylic TCO carbamate **12** and allylic CCO carbamate **11**. Reagents/conditions: (a) *i*. Diphenyl diselenide, H_2O_2, DCM, 0°C; *ii*. MgSO4; *iii*. **7**, 0°C to rt; (b) tBu-OOH, 0°C to rt, 86% over 2 steps; (c) benzyl isocyanate, Et_3N, DCM, rt, 83% (**11**), 77% (**5**); (d) methyl benzoate, hv (254 nm), Et_2O / heptane, rt, 33% (**9**), 22% (**10**).

3.2 Results and discussion

Global acidic deprotection to liberate peptide sequences of their temporary protective groups and resin modalities constitutes a key step in Fmoc SPPS. Depending on the nature of these protective functionalities, varying concentrations of TFA and scavengers are employed for this reaction. In order to achieve the goal of incorporating TCO-modified amino acids into an SPPS-sequence, it was envisioned that the extent and mechanism of TFA-induced isomerization of allylic substituted TCOs would have to be characterized in detail.

Model allylic TCO carbamate **5**[20,29] was synthesized to measure the rate of TFA-induced isomerization with ^{1}H NMR (Scheme 1). Cyclooctenol **6** was obtained from *cis*-cyclooctene (**7**) in a one-pot, two-step procedure involving formation and subsequent oxidation of a hydroxy selenide adduct (**8**).[30,31] Photochemical isomerization of **6** gave a mixture of axial (**9**) and equatorial (**10**) TCO diastereoisomers which were separated using silica gel column chromatography.[20,32] Treatment of **6** and **9** with benzyl isocyanate gave carbamates **11** and **5**, respectively. Exposure of **5** to TFA-H (5% *v/v* in $CDCl_3$) for 30 – 150 minutes, followed by dilution with toluene and concentration *in vacuo* resulted in a progressively isomerized mixture on ^{1}H NMR (Figure 3). While **5** is still the major species after 30 and 60 minutes of incubation (64% and 48% estimated **5** intact, respectively), the spectra of the concentrated mixtures upon prolonged incubation primarily possess *cis*-cyclooctene characteristics, without directly matching reference compound **11**. The latter observation is in agreement with the reactivity of CCOs towards TFA, as described by Nordlander *et al*.[27]

Based on this initial experiment, it was decided that directly monitoring the interaction of **5** and TFA was required to obtain meaningful data. Furthermore, it was reasoned that neutralizing the acidic reaction mixture (e.g. with pyridine)[33] during such an NMR

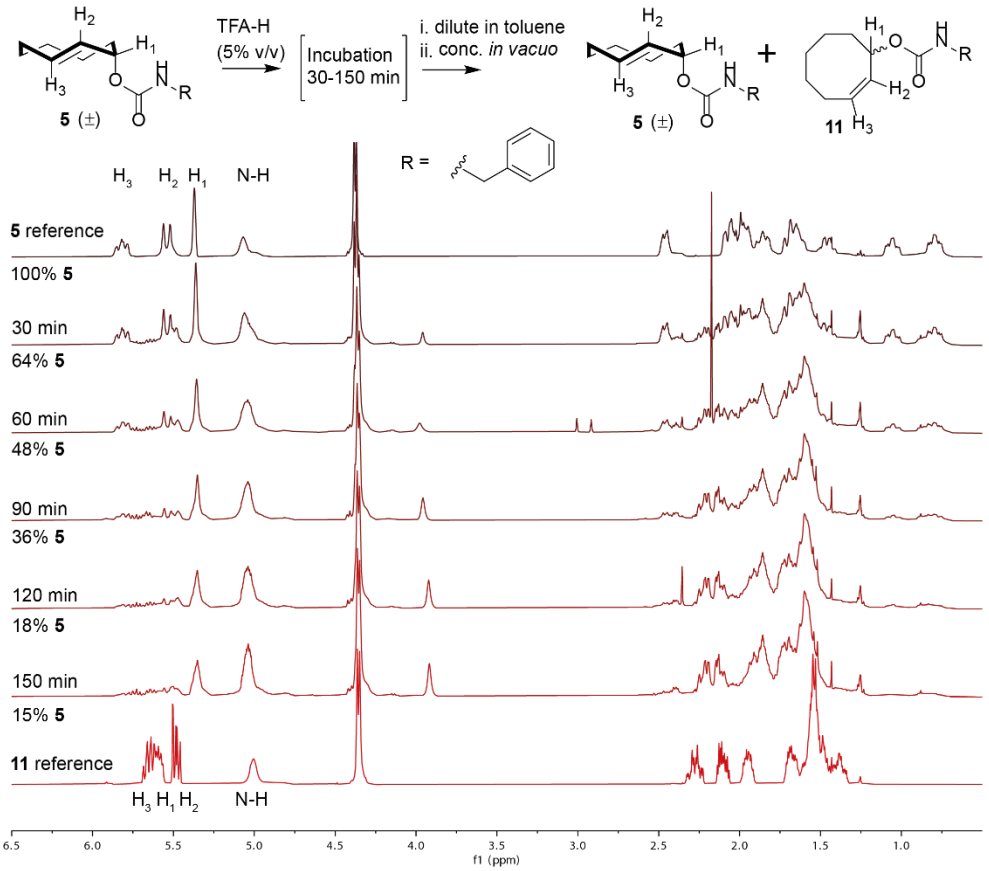

Figure 3 Isomerization/degradation of model compound **5** after incubation (30 – 150 min) with TFA-H (5% *v/v* in $CDCl_3$; 600 µL total volume). After the indicated incubation period, the sample was diluted with toluene (5 mL), concentrated *in vacuo* (40°C) and analyzed with ^{1}H NMR. The stability of **5** was estimated by comparing the H_3 signal (5.90-5.75 ppm) with the methylene signal (4.45-4.30 ppm).

experiment would negate effects of direct concentration and could be translated to Fmoc SPPS procedures.[33]

Addition of TFA-D (5% *v/v* in $CDCl_3$) to **5** led to a clear perturbation of the H_3-signal (δ = 5.8 ppm) towards an overlapping $H_{2\text{-}3}$-signal (δ = 5.7 – 5.4 ppm; Figure 4A). In a similar fashion, peak perturbation and/or broadening was visible for C_1 (δ = 74 ppm), $C_{2\text{-}3}$ (δ = 132 ppm) and C=O (δ = 156 ppm) on ^{13}C-APT NMR (Figure 4B). Other signals in the ^{1}H and ^{13}C NMR spectra for this cationic species showed minor shifts compared to **5**. The overall spectral appearance did not change over the course of the experiment. Administration of pyridine-D_5 (2 equivalents) after 90 minutes directly recovered the spectral appearance of the TCO model compound (**5**), without a significant degree of isomerization (94% stability based on ^{1}H NMR estimations).

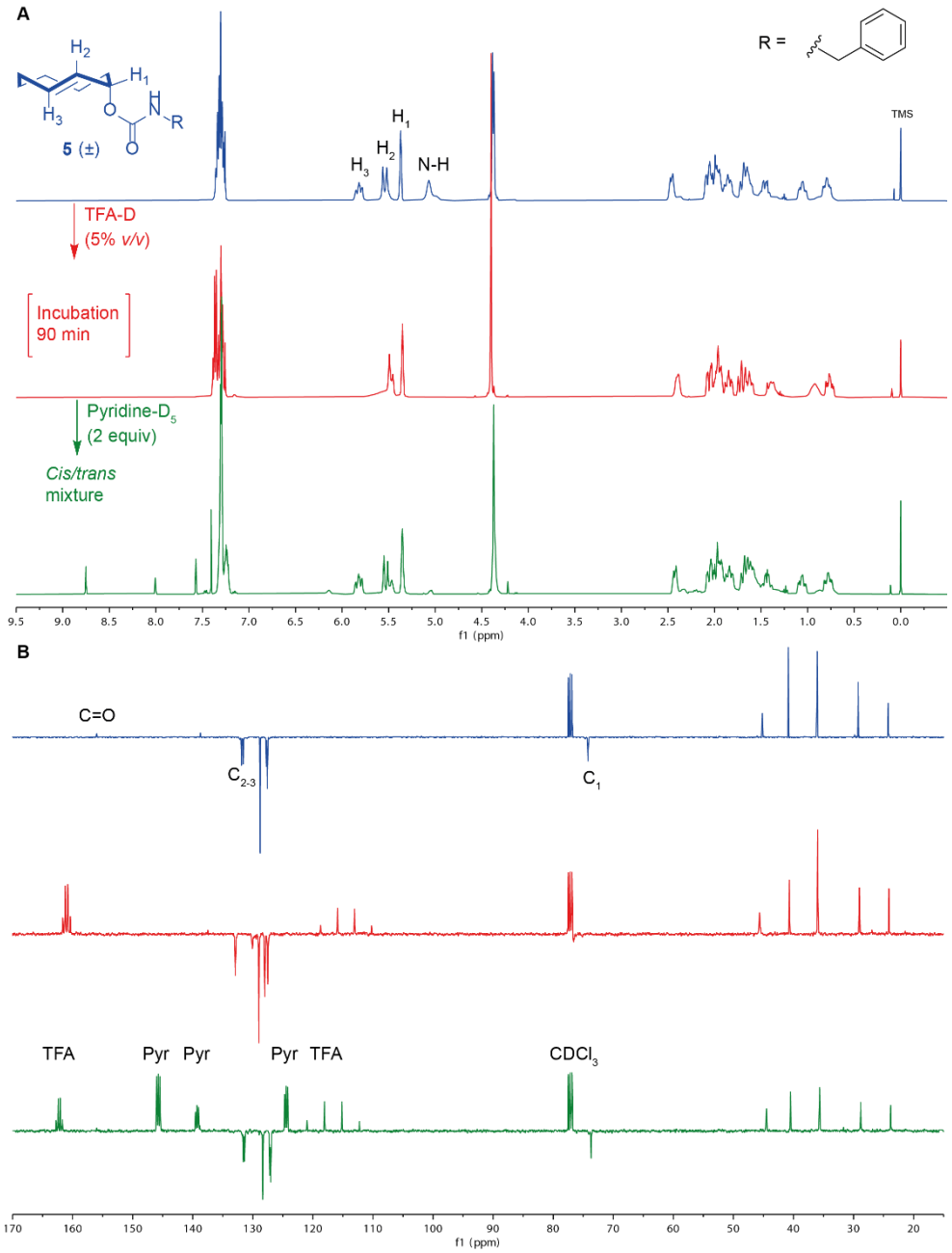

Figure 4 Stacked 1H (A; δ 9.5/-0.5 ppm) and 13C-APT (B; 170/15 ppm) NMR spectra of model TCO carbamate **5** before and upon treatment with TFA-D (5% v/v in CDCl3). Chemical shift perturbation and/or peak broadening is visible in both spectra for characteristic 1H and 13C signals ($H/C_{1\text{-}3}$, C=O). After 90 minutes, the mixture was quenched by adding pyridine-D_5 (2 equiv), recovering the signals for carbamate **5**. The stability of **5** was estimated to be 94% by comparing the H_3 signal (5.90-5.75 ppm) with the methylene signal (4.45-4.30 ppm).

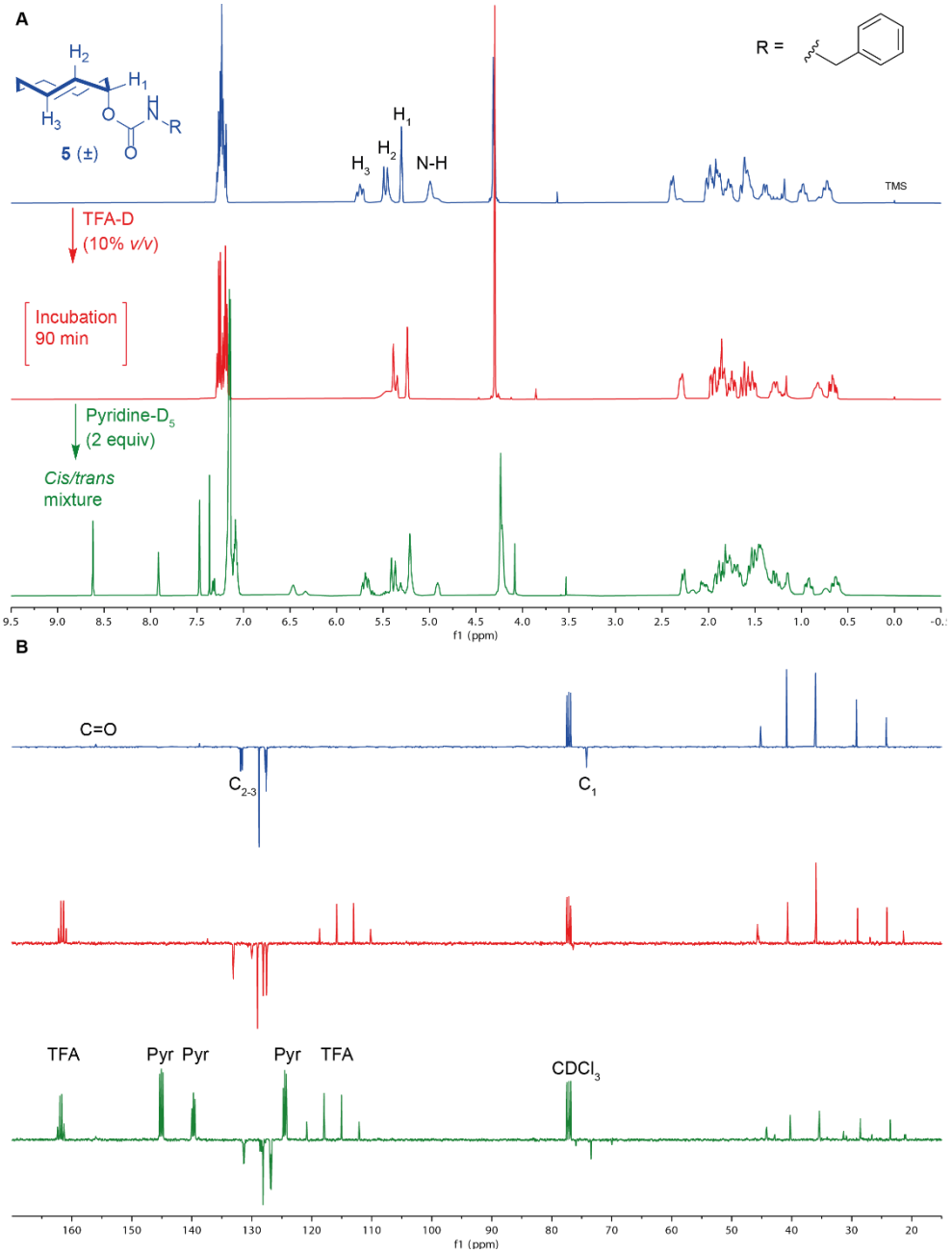

Figure 5 Stacked ^{1}H (A; δ 9.5/-0.5 ppm) and ^{13}C-APT (B; 170/15 ppm) NMR spectra of model TCO carbamate **5** before and upon treatment with TFA-D (10% *v/v* in $CDCl_3$). Chemical shift perturbation and/or peak broadening is visible in both spectra for characteristic ^{1}H and ^{13}C signals ($H/C_{1\text{-}3}$, C=O). After 90 minutes, the mixture was quenched by adding pyridine-D_5 (2 equiv), partially recovering the signals for carbamate **5**. The stability of **5** was estimated to be 75% by comparing the H_3 signal (5.90-5.75 ppm) with the methylene signal (4.45-4.30 ppm).

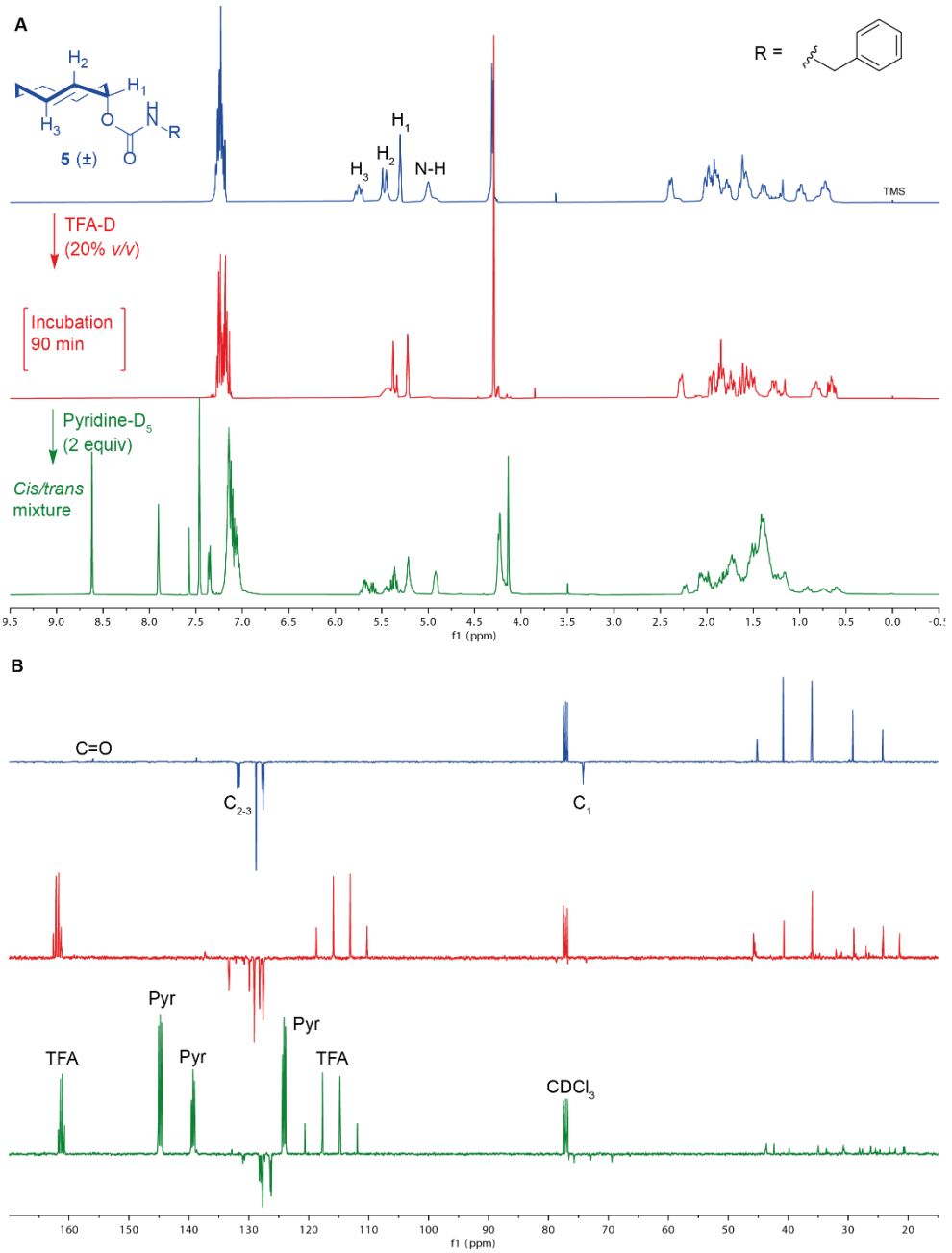

Figure 6 Stacked ^{1}H (A; δ 9.5/-0.5 ppm) and ^{13}C-APT (B; 170/15 ppm) NMR spectra of model TCO carbamate **5** before and upon treatment with TFA-D (20% *v/v* in $CDCl_3$). Chemical shift perturbation and/or peak broadening is visible in both spectra for characteristic ^{1}H and ^{13}C signals ($H/C_{1\text{-}3}$, C=O). After 90 minutes, the mixture was quenched by adding pyridine-D_5 (2 equiv) to obtain a complex, isomerized mixture. The stability of **5** could not be estimated for this time point due to spectral heterogenicity.

This initial experiment was repeated using 10% TFA-D (*v/v* in $CDCl_3$; Figure 5) and 20% TFA-D (*v/v* in $CDCl_3$; Figure 6). In both follow-up experiments, exposure to TFA-D led to the same species, with increasing prevalence of byproducts on ^{13}C-APT (δ = 135-125, 80-70, 45-20 ppm). However, upon quenching with pyridine-D_5, the extent of observed isomerization was more pronounced. While incubation with 10% TFA-D led to an estimated stability of 75% **5**, 20% TFA-D led to a heterogenous spectrum in which the stability for **5** was so low that the data was deemed non extractable.

Based on these data, the existence of a stabilized cationic species was hypothesized to enable (partial) retention of the *trans* olefin configuration during acidic exposure. In an extreme scenario, direct deuteration of **5** with TFA-D likely occurs on C_2 and/or C_3, after which the positive charge can be stabilized by anchimeric assistance of the carbamate moiety. These options were evaluated by computing the (anchimerically) stabilized structures arising from both pathways (protonation on C_2 or C_3) for a model axial TCO carbamate with N-methylation (**12**, Figure 7A). DFT computations reveal that protonation on C_3, with anchimeric assistance as a five-membered ring system, is the most likely stabilized cationic species with a strong preference of 3 kcal mol^{-1}. This is also in agreement with the NMR results presented herein (Figures 4 – 6), where a direct shift of the H_3 signal was observed upon treatment with TFA-D and only a single product was initially observed. Furthermore, it is generally accepted that the formation of a five membered ring would occur faster than the formation of a six-membered ring. It is noteworthy that the computed structure for the cationic species has four carbon atoms in plane and four carbon atoms above that plain. This matches the most stable conformation of *cis*-cyclooctene, as reported by previous DFT studies,[34] but does not explain how the *trans*-configuration is retained or restored upon neutralization. Therefore, the proposed mechanism entails protonation/deuteration of **5** on C_3 and formation of a stabilized cationic species (**13**) by anchimeric assistance of the carbamate moiety towards C_2. This species retains the *trans* configuration and can rearrange into the more stable *cis* configuration (**14**) upon prolonged acidic exposure (Figure 7B).

In order to translate the NMR studies presented herein towards the envisioned Fmoc SPPS strategy, deprotection of the peptide sequence should occur under dilute TFA concentrations (<10% *v/v*). It was reasoned that introduction of the TCO-moiety via selective Lys sidechain deprotections would therefore be limited to allyloxycarbonyl (Alloc) manipulation, as 4-methyltrityl (Mtt) groups are also cleaved under dilute acid.[35] Furthermore, the utilization of a TCO-modified Lys building block could simplify future methodology for TCO-modification of other types of amino acids (Tyr, Ser, Thr) as TCO-ethers.[29,36]

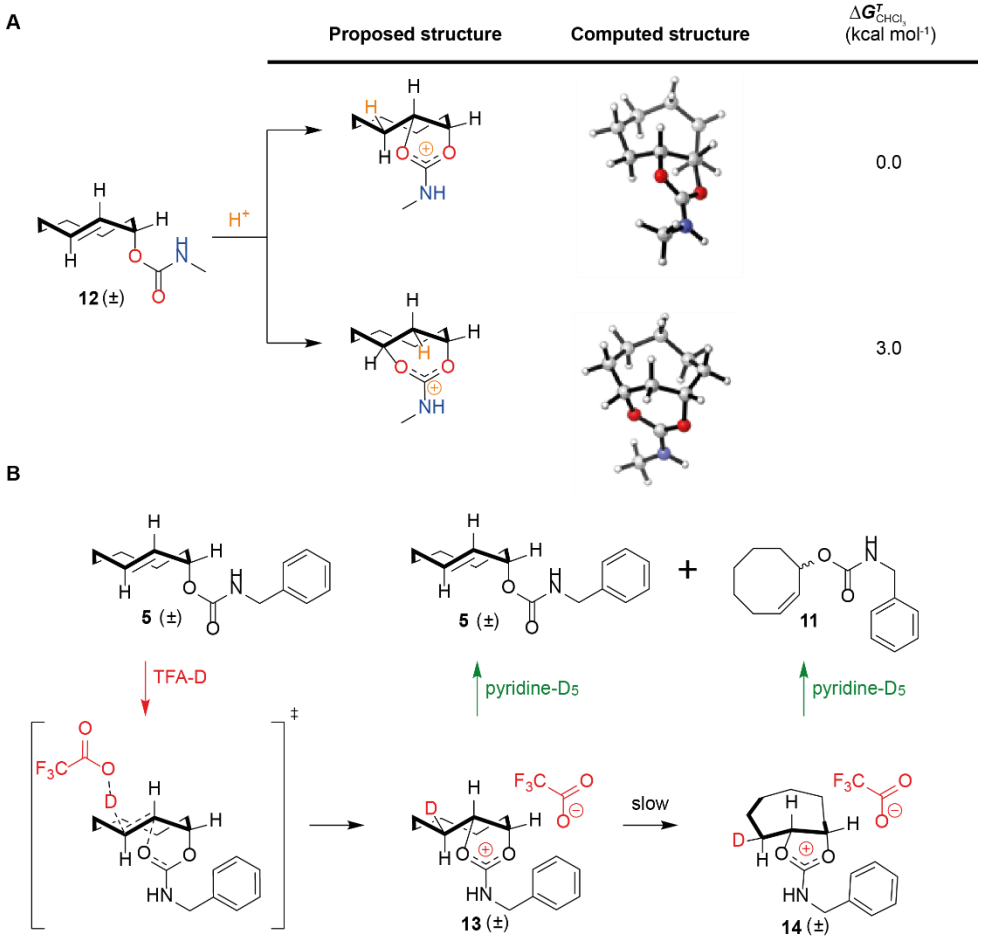

Figure 7 A) Proposed formation of stabilized cationic species upon exposure of TCO-carbamate **12** to TFA. The positive charge created by protonation of C_2 or C_3 can be stabilized by anchimeric assistance of the carbamate moiety, thereby forming either a five- or six-membered ring system. Both structures were computed with DFT, revealing that protonation on C_3 results in the most stable structure by a margin of 3.0 kcal mol^{-1}. Energies are computed at PCM($CHCl_3$)-M06-2X/6-311++G(d,p). B) Mechanistic rationale for the NMR studies presented in this Chapter. Deuteration of **5** on C_3 and anchimeric stabilization on C_2 leads to the formation of a stabilized species cationic species (**13**). From this species, slow isomerization to the *cis*-cyclooctene conformation (**14**) or reformation of **5** (upon neutralization of the acid) can both occur. Calculations were performed by T. Hansen (Leiden University).

Axial TCO carbonates **15** and **16** were obtained by reacting axial TCO **9** with N,N'-disuccinimidyl carbonate and 4-nitrophenyl chloroformate, respectively. Fmoc-Lys(TCO)-OH (**17**)[18,23] was synthesized from Fmoc-Lys-OH (**18**) and carbonates **15** and **16** for incorporation in Fmoc SPPS (Table 1). Conditions derived from procedures

Table 1 Synthesis of Fmoc-Lys(TCO)-OH (**17**) from Fmoc-Lys-OH · HCl (**18**) and axial TCO carbonates **15** and **16**.

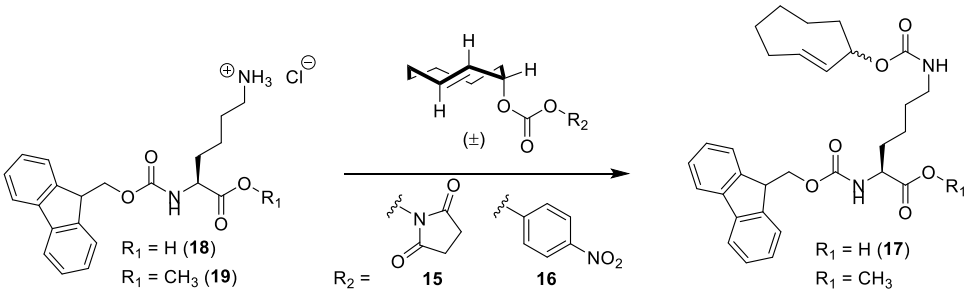

Entry	Lys (eq)	TCO (1 eq)	Scale (mmol)	Base (eq)	Solvent (M)	Time (h)	Yield (%)[a]
1	**18** (1.5)	**15**	0.26	DIPEA (2)	DMF (0.3)	19	36
2	**18** (1.5)	**15**	0.46	DIPEA (2)	DMF (0.3)	48	20
3[b]	**18** (2.0)	**15**	0.50	DIPEA (3)	DMSO (0.1)	19	40
4[c]	**19** (1.5)	**16**	0.29	DIPEA (1.5)	DMSO (0.1)	1	0
5	**19** (1.2)	**16**	0.20	DIPEA (1.2)	DCM (0.2)	4.5	0
6	**18** (1.5)	**16**	0.20	$NaHCO_3$ (3) Na_2CO_3 (1.5)	Dioxane/H_2O 1:1; (0.05)	22	47
7	**18** (2.0)	**16**	0.20	$NaHCO_3$ (4) Na_2CO_3 (2)	Dioxane/H_2O 1:1; (0.1)	19	90
8	**18** (2.0)	**16**	2.0	$NaHCO_3$ (4) Na_2CO_3 (2)	Dioxane/H_2O 1:1; (0.1)	4	90

[a]Isolated yield. [b]Dropwise addition of TCO carbonate **15** over 2 hours. [c]Dropwise addition of DIPEA over 4.5 hours.

by Li *et al*.[23] (entries 1-2) and Nikíc *et al*.[18] (entry 3) were initially investigated using the previously described axial TCO succinimidyl carbonate **15**. The mediocre yield obtained in these entries (20 – 40%) was reduced down to 0% when attempting similar conditions with Fmoc-Lys-OMe (**19**; entries 4-5). Although N_α-Fmoc cleavage is very slow in the presence of tertiary amines such as DIPEA,[37,38] is has been reported that this reaction readily occurs via the ε-amino group of Lysine.[35] Finally, it is conceivable that the absence of a carboxylic acid functionality (entries 4-5) further enhanced this deprotection. The isolated yield of Fmoc-Lys(TCO)-OH (**17**) was increased up to 90% by switching to a dioxane/H_2O (1:1 *v/v*) solvent system in which a mixture of sodium bicarbonate and sodium carbonate was employed as base (entry 7). This optimized procedure was also executed on mmol scale in which the reaction reached completion within 4 hours (entry 8).

Fmoc-Lys(TCO)-OH (**17**) was evaluated as a building block for Fmoc SPPS in the direct synthesis of TCO-modified SIINFEKL (Figure 8A). The design and application in chemical immunology for TCO modification of this peptide sequence is described in Chapter 4. C-terminal loading was accomplished using a Tentagel resin with a TFA labile (≥ 5% *v/v* in DCM) AC linker (3-methoxy-4(hydroxymethyl)phenoxyacetic acid; Rapp polymere). Ser and Glu were incorporated with trityl (Trt; 1 - 5% TFA in DCM, *v/v*)[39] and 2-phenylisopropyl ester (2-PhiPr; 2 – 4% TFA in DCM, *v/v*)[40] protective groups, respectively. The recently introduced 4-monomethoxytrityl (MMt) protection of Asn was chosen over conventional trityl (Trt; 95% TFA in DCM, *v/v*) protection.[41]

After verifying successful assembly of the peptide sequence using an analytical deprotection with TFA/H_2O/TIS (95/2.5/2.5, *v/v*), the resin bound peptide (**20**) was subjected to various deprotection conditions (5/10/20% TFA in DCM, 2% TIS, *v/v*) for 60 minutes. Deprotection mixtures were neutralized in MeOH/pyridine (2 equivalents), concentrated *in vacuo* and treated with tetrazine **21** to enable estimation of the *cis*/*trans* ratio by LC/MS analysis. The results revealed that, in contrast to the complete deprotection of the Ser and Glu residues, the Asn residue only approached full deprotection at 20% TFA (*v/v*). Furthermore, an increasing degree of cyclooctene carbamate hydrolysis was observed for higher TFA concentrations. The peptides detected with the cyclooctene modality retained 45% (5% TFA, 2% TIS, *v/v*) to 9% (20% TFA, 2% TIS, *v/v*) of their *trans* olefin bond.

Taken together, these results indicate the deprotection of (Lys)-TCO-modified peptides from solid support should preferably constitute short exposure times with low TFA concentrations, thereby minimizing the hydrolysis and isomerization of the TCO-carbamate moiety. The feasibility of this approach was recently demonstrated by synthesizing a TLR-2 agonist with N-terminal TCO carbamate modification using Fmoc SPPS.[42] In this case, exposing the construct for 15 min to 5% TFA, 2.5% TIS, 2.5% H_2O in DCM (*v/v*), followed by HPLC purification, led to sufficient quantity of the desired *trans*-product.[42]

Side chain protecting groups employed for Fmoc building blocks are to be carefully selected for this strategy. In case of the SIINFEKL sequence, and C/N-terminally extended derivatives thereof, the abovementioned deprotection conditions could be feasible by incorporating the Asn residue without a sidechain protecting group. β-Cyano-aniline formation, by dehydration of Fmoc-Asn-OH during carboxylic acid activation,[43] can be minimized by employing 1-hydroxy-1H-benzotriazole (HOBt) as an additive for carbodiimide procedures or by use of activated ester derivatives of Fmoc-Asn-OH.[44,45] For long sequences, where the reduced solubility of exposed Asn sidechains is more relevant, the development of a highly acid labile (≤ 5% TFA in DCM,

A

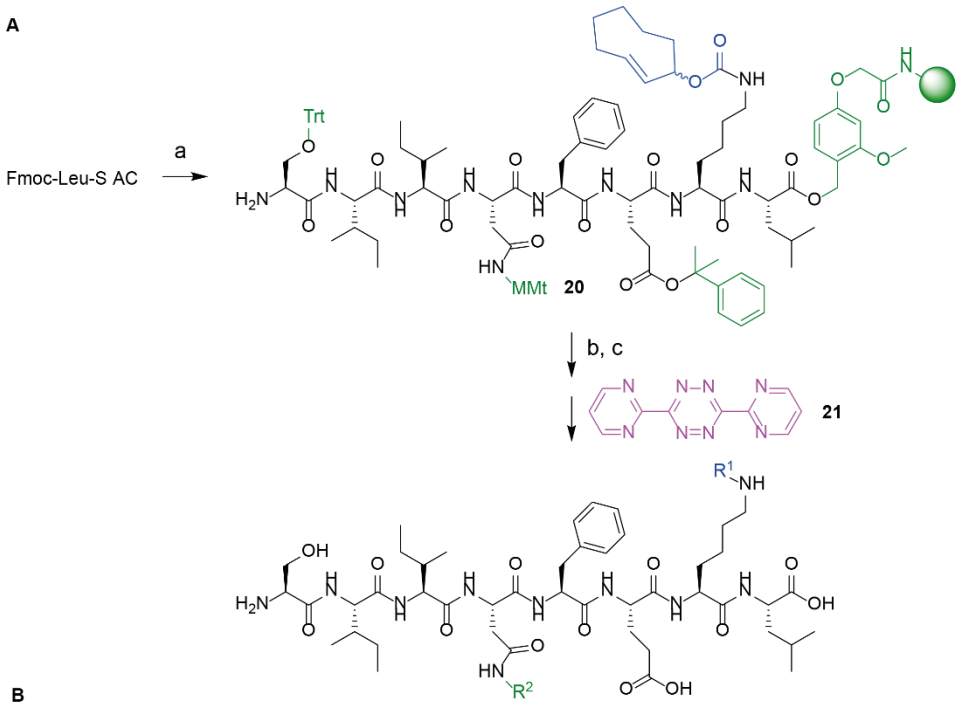

B

Deprotection conditions ⟶	5% TFA, 2% TIS	10% TFA, 2% TIS	20% TFA, 2% TIS
Fragment groups	Relative signal	Relative signal	Relative signal
R^1 = 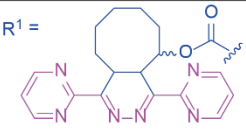 R^2 = H R^2 = MMt	1.0	1.0	1.0
	% *trans*: 45	% *trans*: 34	% *trans*: 9
R^1 = 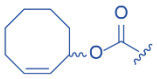 R^2 = H R^2 = MMt	1.23	1.94	10.71
R^1 = H R^2 = H R^2 = MMt	0.56	0.61	2.80

Figure 8 A) Incorporation of Fmoc-Lys(TCO)-OH (**17**) in Fmoc SPPS. Reagents/conditions: (a) Fmoc SPPS from Fmoc-Leu-S AC (tentagel resin) employing building blocks: **17**, Fmoc-Glu(2-PhiPr)-OH, Fmoc-Phe-OH, Fmoc-Asn(MMt)-OH, Fmoc-Ile-OH (x2) and Fmoc-Ser(Trt)-OH; (b) 5-20% TFA, 2% TIS in DCM (*v/v*), 1 h; (c) pyridine (2 equiv) in MeOH. B) Summary of LC/MS analyses of the deprotection mixtures. Analytical samples were treated with tetrazine **21** prior to LC/MS analysis to allow discrepancy between *cis* and *trans*-cyclooctene moieties. Relative signals of the total ion count (TIC) were calculated for the fragment groups displayed.

v/v) protective group for Asn, such as 4,4'-dimethoxytrityl (DMT), could be of importance.

3.3 Conclusions

In conclusion, approaches towards an Fmoc SPPS-based strategy for TCO-modified peptide synthesis is described. TFA induced isomerization of a model axial allylic substituted TCO carbamate was studied using ^{1}H and ^{13}C NMR. The results confirmed that global deprotection of a peptide sequence should occur under dilute TFA concentrations (< 10% *v/v*). Preferential protonation on C_3 and anchimeric assistance of the carbamate moiety towards C_2 was hypothesized to account for the stability of the cationic species formed under these acidic conditions. Optimized synthesis of an Fmoc-Lys(TCO)-OH building block was followed by its incorporation in the SIINFEKL peptide sequence on solid support. Global deprotection of this sequence under dilute TFA concentrations (5% *v/v*, 60 minutes) led to substantial TCO isomerization and carbamate hydrolysis, indicating that further optimization of this deprotection step is required. An alternative synthetic strategy, featuring solution phase coupling of the TCO moiety to peptide sequences after Fmoc SPPS, was explored in Chapter 4 as a consequence of the results described in this Chapter.

3.4 Experimental procedures

General methods: Commercially available reagents and solvents were used as received. Moisture and oxygen sensitive reactions were performed under N_2 atmosphere (balloon). DCM, toluene, dioxane and Et_2O were stored over (flame-dried) 4 Å molecular sieves (8-12 mesh). MeOH was stored over (flame-dried) 3 Å molecular sieves. DIPEA and Et_3N were stored over KOH pellets. TLC analysis was performed using aluminum sheets, pre-coated with silica gel (Merck, TLC Silica gel 60 F_{254}). Compounds were visualized by UV absorption (λ = 254 nm), by spraying with either a solution of $KMnO_4$ (20 g/L) and K_2CO_3 (10 g/L) in H_2O, a solution of $(NH_4)_6Mo_7O_{24} \cdot 4H_2O$ (25 g/L) and $(NH_4)_4Ce(SO_4)_4 \cdot 2H_2O$ (10 g/L) in 10% H_2SO_4, 20% H_2SO_4 in EtOH, or phosphomolybdic acid in EtOH (150 g/L), where appropriate, followed by charring at ca. 150°C. Column chromatography was performed on Screening Devices b.v. Silica Gel (particle size 40-63 μm, pore diameter 60 Å). Celite Hyflo Supercel (Merck) was used to impregnate the reaction mixture prior to silica gel chromatography when indicated. ^1H, ^{13}C APT, ^1H COSY, HSQC and HMBC spectra were recorded with a Bruker AV-400 (400/100 MHz) or AV-500 (500/125 MHz) spectrometer. Chemical shifts are reported as δ values (ppm) and were referenced to tetramethylsilane (δ = 0.00 ppm) or the residual solvent peak as internal standard. *J* couplings are reported in Hz. LC-MS analysis was performed on a Finnigan Surveyor HPLC system (detection at 200-600 nm) with an analytical C_{18} column (Gemini, 50 x 4.6 mm, 3 μm particle size, Phenomenex) coupled to a Finnigan LCQ Advantage MAX ion-trap mass spectrometer (ESI^+). The applied buffers were H_2O, MeCN and 1.0% TFA in H_2O (0.1% TFA end concentration). The method used was: 10% → 90% MeCN, 13.5 min (0→0.5 min: 10% MeCN; 0.5→8.5 min: gradient time; 8.5→10.5 min: 90% MeCN; 10.5→13.5 min: 90% → 10% MeCN). The synthesis of tetrazine **21** is described in Chapter 4 and a recent publication.[24]

Photoisomerization methods: General guidelines were followed as described by Royzen *et al*.[32] Photochemical isomerization was performed using a Southern New England Ultraviolet Company Rayonet reactor (model RPR-100) equipped with 16 bulbs (part number RPR-2537A, λ = 254 nm). Photolysis was performed in a 1500 mL quartz flask (Southern New England Ultraviolet Company; part number RQV-323). A HPLC pump (Jasco; model PU-2088 Plus) was used to circulate solvent through the photolysis apparatus at the indicated flow rate. An empty solid load cartridge with screw cap, frits, O-ring and end tips (40 g; SD.0000.040; iLOK™, Screening Devices b.v.) was manually loaded with the specified silica gel to function as the stationary phase.

Computational methods: The density functional theory (DFT) computations were performed using Gaussian 09 rev D.01. For all computation the hybrid functional B3LYP–D3(BJ) and M06–2X were used for geometry optimization and energy calculation respectively. In terms of the basis set, 6–31+G(d) was used for geometry optimization and 6–311++G(d,p) was used for energy calculation. The internally defined super-fine grid size was used (SCF=tight, Int=veryfinegrid), which is a pruned 175,974 grid for first-row atoms and a 250,974 grid for all other atoms. Geometries were optimized without symmetry constraints. All calculated stationary points have been verified by performing a vibrational analysis, to be energy minima (no imaginary frequencies). Solvation in chloroform was taken into account in the computations using the PCM implicit solvation model. Solvent effects were explicitly used in the solving of the SCF equations

and during the optimization of the geometry and the vibrational analysis. The ring dihedral angles were constrained for all conformations. The optimized structures were illustrated using CYLview.

The denoted free Gibbs energy was calculated using Equation S1, in which ΔE_{gas} is the gas-phase energy (electronic energy), $\Delta G^{T}_{\text{gas,QH}}$ (T = 293.15 K, p = 1 atm., C = 1 M) is the sum of corrections from the electronic energy to the free Gibbs energy in the quasi-harmonic oscillator approximation, including zero-point-vibrational energy, and ΔG_{solv} is their corresponding free solvation Gibbs energy. The $\Delta G^{T}_{\text{gas,QH}}$ was computed using the quasi-harmonic approximation in the gas phase according to the work of Truhlar.[46] The quasi-harmonic approximation is the same as the harmonic oscillator approximation except that vibrational frequencies lower than 100 cm^{-1} were raised to 100 cm^{-1} as a way to correct for the breakdown of the harmonic oscillator model for the free energies of low-frequency vibrational modes.[46]

$$\Delta G^{T}_{\text{H2O}} = \Delta E_{\text{gas}} + \Delta G^{T}_{\text{gas,QH}} + \Delta G_{\text{solv}} \qquad \text{(Eq. S1)}$$

$$= \Delta G^{T}_{\text{gas}} + \Delta G_{\text{solv}}$$

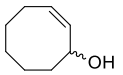

Cyclooctenol 6: Synthesis was performed according to literature references.[30,31] A solution of diphenyl diselenide (10.0 g, 32.0 mmol, 1.5 equiv) in DCM (100 mL) was cooled to 0°C (ice bath) under an argon atmosphere before adding hydrogen peroxide solution (35% *w/w*, 2.85 mL, 32.6 mmol, 1.5 equiv) dropwise. The reaction mixture was stirred for 75 min before adding magnesium sulfate hydrate (11 g). The resulting suspension was stirred for 60 min before removing the ice bath and adding (Z)-cyclooctene (**7**, 2.80 mL, 21.46 mmol, 1.0 equiv). The reaction mixture was stirred for 22 h at room temperature, after which conversion to the intermediate hydroxyl selenide adduct (**8**) was shown using TLC (R_f = 0.4 (pentane)). The reaction mixture was cooled to 0°C (ice bath) before adding *tert*-butyl hydroperoxide (~5.5 M in decane, 20.73 mL, 114 mmol, 5.3 equiv) dropwise. The ice bath was removed and the reaction mixture was stirred for > 20 h at room temperature under an argon atmosphere, resulting in an orange solution with a colorless precipitate. The reaction mixture was filtered, the residue was washed with Et_2O and the orange filtrate was concentrated *in vacuo*. The crude oil was redissolved in Et_2O (~150 mL) and washed with Na_2CO_3 (5% *w/w*, 2 x 100 mL), H_2O (100 mL), Fe_2SO_4 (10% *w/w*, 2 x 100 mL), H_2O (100 mL), $NaHCO_3$ (sat., 100 mL), H_2O (100 mL) and brine (100 mL). The organic layer was then dried over $MgSO_4$, filtered and concentrated *in vacuo*. The crude product was purified by silica gel chromatography (15% → 20% Et_2O in pentane). Cyclooctenol **6** (2.34 g, 18.54 mmol, 86%) was collected as a yellow oil: R_f = 0.3 (20% Et_2O in pentane); ^1H NMR (400 MHz, $CDCl_3$) δ 5.60 (dddd, *J* = 10.3, 8.5, 7.0, 1.4 Hz, 1H), 5.52 (ddd, *J* = 10.8, 6.6, 1.0 Hz, 1H), 4.69 – 4.61 (m, 1H), 2.22 – 2.02 (m, 2H), 1.95 – 1.86 (m, 1H), 1.81 (s, 1H), 1.69 – 1.32 (m, 7H); ^{13}C NMR (101 MHz, $CDCl_3$) δ 135.1, 128.7, 69.6, 38.7, 29.2, 26.4, 26.0, 23.8. Spectroscopic data was in agreement with literature.[31]

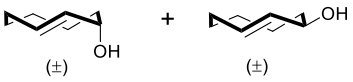

***Trans*-cyclooctenol; axial diastereoisomer (9) and equatorial diastereoisomer (10):** Synthesis was performed according to literature references.[20,32] Cyclooctenol **6** (1.00 g, 7.92 mmol, 1.0 equiv) was irradiated (λ = 254 nm) for 20 h in the presence of methyl benzoate (2.60 ml, 20.60 mmol, 2.6 equiv) in a quartz flask containing a solution of Et_2O in heptane (10% *v/v*, 500 mL). During irradiation, the reaction mixture was continuously circulated over a column (40 g size, containing dry silica and 17 g of $AgNO_3$ impregnated silica[32] (10% w/w, containing ca. 10 mmol $AgNO_3$, 1.26 equiv)) at a flowrate of 40 mL/min. The column was placed in the dark and shielded with aluminum foil during the irradiation. Absence of **6** from the reaction mixture was shown with ^1H NMR and the column was flushed with Et_2O in heptane (10% *v/v*, 600 mL) before drying over a stream of air. Next, the contents of the column were emptied into an Erlenmeyer flask containing NH_4OH (sat., 200 mL) and DCM (200 mL). The biphasic mixture was stirred for ~ 1 h before filtration of the silica gel. The organic layer was separated and the aqueous layer was extracted with DCM (200 mL). The combined organic layers were washed with H_2O (100 mL), dried over $MgSO_4$, filtered and concentrated *in vacuo*. The crude isomeric mixture was separated and purified by silica gel chromatography (15% Et_2O in pentane; isocratic). The axial product (**9**, 328 mg, 2.60 mmol, 33%) was obtained as an oil: R_f = 0.4 (20% Et_2O in pentane); ^1H NMR (400 MHz, $CDCl_3$) δ 5.96 (ddd, *J* = 15.5, 11.0, 3.5 Hz, 1H), 5.58 (dd, *J* = 16.5, 2.2 Hz, 1H), 4.61 (br s, 1H), 2.52 – 2.45 (m, 1H), 2.08 – 2.00 (m, 1H), 1.99 – 1.92 (m, 2H), 1.90 – 1.80 (m, 1H), 1.72 – 1.46 (m, 4H), 1.17 – 1.06 (m, 1H), 0.82 – 0.71 (m, 1H); ^{13}C NMR (101 MHz, $CDCl_3$) δ 135.3, 130.7, 71.4, 43.3, 36.2, 36.0, 29.3, 23.3. The equatorial product (**10**, 217 mg, 1.72

mmol, 22%) was obtained as an oil: R_f = 0.2 (20% Et_2O in pentane); ^1H NMR (400 MHz, $CDCl_3$) δ 5.71 – 5.61 (m, 1H), 5.54 (dd, *J* = 16.2, 9.1 Hz, 1H), 4.26 (td, *J* = 9.5, 5.6 Hz, 1H), 2.43 – 2.36 (m, 1H), 2.19 – 2.11 (m, 1H), 2.02 – 1.72 (m, 5H), 1.54 – 1.34 (m, 2H), 0.94 – 0.84 (m, 1H), 0.81 – 0.70 (m, 1H). ^{13}C NMR (101 MHz, $CDCl_3$) δ 135.8, 131.8, 76.8, 44.3, 35.9, 35.4, 29.1, 27.7. Spectroscopic data was in agreement with literature.[20]

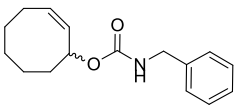

CCO carbamate 11: Cyclooctenol **6** (379 mg, 3.0 mmol, 1.0 equiv) was dissolved in anhydrous DCM (20 mL) under N_2. Benzyl isocyanate (1.16 ml, 9.36 mmol, 3.12 equiv) and Et_3N (150 µl, 1.07 mmol, 0.36 equiv) were subsequently added. The reaction mixture was stirred at room temperature for 72 h, impregnated with Celite and concentrated *in vacuo*. The impregnated crude product was purified by silica gel chromatography (10% Et_2O in pentane) to obtain CCO carbamate **11** (643 mg, 2.48 mmol, 83 %) as white solid: ^1H NMR (400 MHz, $CDCl_3$) δ 7.39 – 7.24 (m, 5H), 5.70 – 5.62 (m, 1H), 5.63 – 5.56 (m, 1H), 5.48 (ddd, *J* = 10.8, 7.0, 1.3 Hz, 1H), 4.96 (br s, 1NH), 4.36 (d, *J* = 5.9 Hz, 2H), 2.35 – 2.22 (m, 1H), 2.16 – 2.05 (m, 1H), 2.00 – 1.90 (m, 1H), 1.73 – 1.63 (m, 1H), 1.62 – 1.45 (m, 5H), 1.44 – 1.32 (m, 1H); ^{13}C NMR (101 MHz, $CDCl_3$) δ 156.3, 138.8, 131.2, 129.6, 128.7 (x2), 127.7, 127.5 (x2), 73.1, 45.1, 35.5, 28.9, 26.4, 26.0, 23.5.

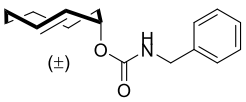

Axial TCO carbamate 5: Procedure was modified from existing literature.[20] Axial TCO-OH **9** (252 mg, 2.0 mmol, 1.0 equiv) was dissolved in anhydrous DCM (14 mL) under N_2. Benzyl isocyanate (771 µl, 6.24 mmol, 3.12 equiv) and Et_3N (100 µl, 0.72 mmol, 0.36 equiv) were added before shielding the reaction mixture with aluminum foil. The reaction mixture was stirred at room temperature for 72 h, impregnated with Celite and concentrated *in vacuo*. The impregnated crude product was purified by silica gel chromatography (5% Et_2O in pentane → 20% Et_2O in pentane) to obtain axial TCO carbamate **5** (401 mg, 1.55 mmol, 77 %) as white solid: ^1H NMR (400 MHz, $CDCl_3$) δ 7.43 – 7.19 (m, 5H), 5.92 – 5.73 (m, 1H), 5.54 (d, *J* = 16.5 Hz, 1H), 5.37 (s, 1H), 5.06 (br s, 1NH), 4.38 (d, *J* = 6.0 Hz, 2H), 2.55 – 2.29 (m, 1H), 2.13 – 1.91 (m, 3H), 1.91 – 1.77 (m, 1H), 1.75 – 1.56 (m, 2H), 1.54 – 1.39 (m, 1H), 1.13 – 0.98 (m, 1H), 0.92 – 0.70 (m, 1H); ^{13}C NMR (101 MHz, $CDCl_3$) δ 156.0, 138.7, 131.9, 131.6, 128.8 (x2), 127.8, 127.6 (x2), 74.2, 45.2, 40.9, 36.1, 36.0, 29.2, 24.2. Spectroscopic data was in agreement with literature.[20]

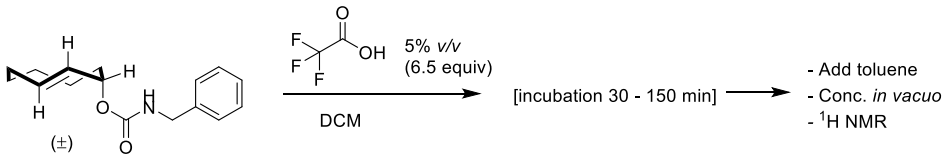

5% *v/v* TFA in DCM, incubation experiment (30 – 150 min) with axial TCO carbamate (5): Axial TCO carbamate **5** (105 mg, 0.40 mmol, 1.0 equiv) was dissolved in anhydrous DCM (3.8 mL) under N_2. The flask was tightly wrapped with parafilm, shielded with aluminum foil and placed in the dark. Subsequently, TFA-H (200 µL, 2.60 mmol, 6.5 equiv) was added, obtaining a 0.1 M solution of **5** in 5% TFA-H (*v/v* in DCM). The solution was stirred at room temperature for 2.5 h during which a sample (600 µL) was taken every 30 min. Samples were diluted with toluene (5 ml), concentrated *in vacuo* (40°C) and analyzed by ^1H NMR.

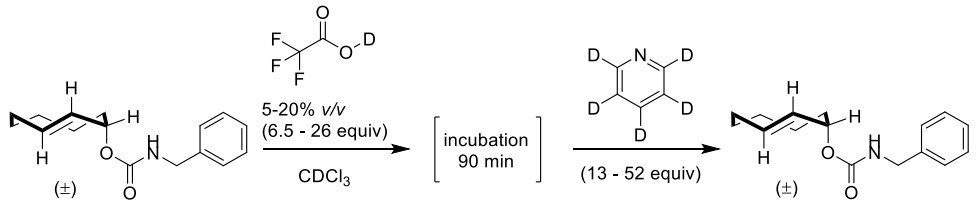

Stability NMR experiment with axial TCO carbamate 5 - 5-20% *v/v* TFA-D in DCM - incubation 90 min - quenching with pyridine D_5: Axial TCO-carbamate **5** (15.5 mg, 60 µmol, 1.0 equiv) was dissolved in $CDCl_3$ (570/540/480 µL) in an NMR tube. After measuring a reference spectrum (^{1}H NMR), TFA-D (30µL, 0.39 mmol, 6.5 equiv; 60µL, 0.78 mmol, 13 equiv; 120µL, 1.56 mmol, 26 equiv) was added to obtain a 0.1 M solution of **5** in 5/10/20% TFA-D (*v/v* in $CDCl_3$). The mixture was vortexed for 1 min, and subsequently characterized with NMR (^{1}H, ^{13}C, COSY, HSQC). After 90 min, the mixture was neutralized by adding pyridine-D_5 (63 µL, 0.78 mmol, 13 equiv; 126µL, 1.56 mmol, 26 equiv; 252µL, 3.12 mmol, 52 equiv), vortexed for 1 min and characterized with NMR (^{1}H, ^{13}C, COSY, HSQC).

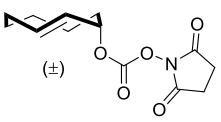

Axial TCO carbonate 15: Axial TCO-OH **9** (380 mg, 2.98 mmol, 1.0 equiv) was dissolved in anhydrous MeCN (15 mL) under N_2. N,N'-disuccinimidyl carbonate (1.53 g, 5.96 mmol, 2.0 equiv) and DIPEA (1.04 mL, 5.96 mmol, 2.0 equiv) were added and the reaction mixture, the reaction mixture was shielded with aluminium foil and stirred at room temperature for 120 h. The reaction mixture was concentrated *in vacuo* and the crude product was purified by silica gel chromatography (20% EtOAc in pentane; isocratic) to obtain axial TCO carbonate **15** (710 mg, 2.66 mg, 89%) as a crystalline solid: R_f = 0.2 (20% EtOAc in pentane); ^{1}H NMR (400 MHz, $CDCl_3$) δ 5.97 (ddd, J = 15.6, 11.0, 3.6 Hz, 1H), 5.50 (dd, J = 16.5, 2.1 Hz, 1H), 5.40 (br s, 1H), 2.84 (s, 4H), 2.57 – 2.48 (m, 1H), 2.27 – 2.17 (m, 2H), 2.10 – 1.95 (m, 2H), 1.95 – 1.84 (m, 1H), 1.82 – 1.65 (m, 2H), 1.61 – 1.47 (m, 1H), 1.20 – 1.08 (m, 1H), 0.88 – 0.75 (m, 1H); ^{13}C NMR (101 MHz, CDCl3) δ 168.8 (x2), 150.8, 133.6, 128.4, 81.2, 40.5, 36.2, 35.9, 29.0, 25.6 (x2), 23.9.

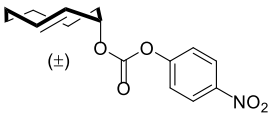

Axial TCO carbonate 16: Axial TCO-OH **9** (330 mg, 2.63 mmol, 1.0 equiv) was dissolved in anhydrous DCM (12 mL) under N_2. Anhydrous pyridine (0.64 mL, 7.89 mmol, 3.0 equiv) was added before cooling the reaction mixture to 0°C (ice-bath). 4-Nitrophenyl chloroformate (1.27 g, 6.32 mmol, 2.4 equiv) was added, the reaction mixture was shielded with aluminium foil, stirred for 60 h and allowed to warm to room temperature. The reaction mixture was diluted with H_2O (15 mL) and the aqueous layer was extracted with Et_2O (3 x 30 mL). The combined organic layers were washed with HCl (1 M, 2 x 20 mL), $NaHCO_3$ (satd., 2 x 30 mL) and brine (60 mL), dried over $MgSO_4$, filtered and concentrated *in vacuo*. The crude product was purified by silica gel chromatography (5% Et_2O in pentane, isocratic) to obtain axial TCO carbonate **16** (710 mg, 2.44 mmol, 93%) as a crystalline solid: R_f = 0.2 (5% Et_2O in pentane); ^{1}H NMR (400 MHz, $CDCl_3$) δ 8.30 – 8.24 (m, 2H), 7.43 – 7.36 (m, 2H), 5.97 (ddd, *J* = 15.7, 11.2, 3.6 Hz, 1H), 5.57 (dd, *J* = 16.5, 2.2 Hz, 1H), 5.43 (s, 1H), 2.56 – 2.48 (m, 1H), 2.26 – 2.18 (m, 1H), 2.12 – 1.97 (m, 2H), 1.97 – 1.86 (m, 1H), 1.85 – 1.67 (m, 2H), 1.59 – 1.48 (m, 1H), 1.22 – 1.11 (m, 1H), 0.88 – 0.78 (m, 1H); ^{13}C NMR (101 MHz, $CDCl_3$) δ 155.7, 151.8, 145.4, 133.2, 129.5, 125.4 (x2),

121.9 (x2), 78.9, 40.6, 36.1, 36.0, 29.0, 24.1. Spectroscopic data was in agreement with literature.[20]

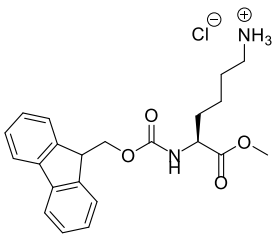

Fmoc-Lys-OMe · HCl (19): Fmoc-Lys-OH • HCl (**18**, 2.02 g, 5.0 mmol, 1.0 equiv) was dissolved in anhydrous MeOH (15 mL) under N_2. The solution was cooled to 0°C (ice-bath) before dropwise addition of $SOCl_2$ (766 µL, 10.5 mmol, 2.1 equiv) over 15 min. The reaction mixture was stirred for 20 min at 0°C and was subsequently stirred for 2 h at 50°C (oil-bath). The reaction mixture was concentrated *in vacuo* and co-evaporated with MeOH (3 x 10 mL) to obtain methyl ester **19** (1.83 g, 4.37 mmol, 87%) as an orange, foamy solid: R_f = 0.4 (20% MeOH in DCM); ^{1}H NMR (400 MHz, DMSO-d_6) δ 7.93 (br s, 3NH), 7.90 (d, *J* = 7.5 Hz, 2H), 7.80 (d, *J* = 7.7 Hz, 1NH), 7.72 (dd, *J* = 7.5, 4.5 Hz, 2H), 7.42 (t, *J* = 7.4 Hz, 2H), 7.33 (t, *J* = 7.3 Hz, 2H), 4.37 – 4.26 (m, 2H), 4.26 – 4.18 (m, 1H), 4.06 – 3.95 (m, 1H), 3.63 (s, 3H), 2.82 – 2.62 (m, 2H), 1.75 – 1.58 (m, 2H), 1.59 – 1.45 (m, 2H), 1.43 – 1.26 (m, 2H); ^{13}C NMR (101 MHz, DMSO-d_6) δ 172.9, 156.2, 143.7 (x2), 140.7 (x2), 127.7 (x2), 127.1 (x2), 125.2, 125.2, 120.2 (x2), 65.6, 53.7, 52.0, 46.6, 38.4, 30.0, 26.4, 22.4. Spectroscopic data was in agreement with literature.[47]

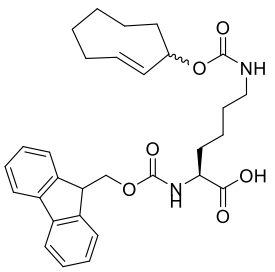

Fmoc-Lys(TCO)-OH (17): Fmoc-Lys-OH • HCl (**18**, 162 mg, 0.40 mmol, 2.0 equiv) was dissolved in H_2O (0.5 mL) before adding a solution of $NaHCO_3$ (67 mg, 0.80 mmol, 4.0 equiv) and Na_2CO_3 (42 mg, 0.40 mmol, 2.0 equiv) in H_2O (0.5 mL). The mixture was briefly cooled towards 0°C (ice-bath) before adding a solution of axial TCO carbonate **16** (58 mg, 0.2 mmol, 1.0 equiv) in dioxane (1 mL). The yellow reaction mixture was shielded with aluminium foil, stirred for 19 h and allowed to warm to room temperature. The reaction mixture was cooled (ice-bath), quenched with HCl (2% *w/w*, 4 mL) and partially concentrated *in vacuo* (40°C, 100 mbar). The aqueous layer was extracted with EtOAc (3 x 5 mL); the combined organic layers were dried over $MgSO_4$, filtered, impregnated with Celite and concentrated *in vacuo*. The crude, impregnated product was purified by silica gel chromatography (20% Et_2O in pentane → DCM → 0.5% MeOH, 1% AcOH in DCM) to obtain the diastereomeric mixture Fmoc-Lys(TCO)-OH (**17$_A$ + 17$_B$**, 94 mg, 0.18 mmol, 90%) as a solid: R_f = 0.15 (2% MeOH, 1% AcOH in DCM); ^{1}H NMR (400 MHz, MeOD/$CDCl_3$; 9:1) δ 7.74 (d, *J* = 7.5 Hz, 2H), 7.63 (t, *J* = 7.1 Hz, 2H), 7.36 (t, *J* = 7.4 Hz, 2H), 7.28 (td, *J* = 7.4, 1.0 Hz, 2H), 5.81 (ddd, *J* = 15.7, 11.0, 3.6 Hz, 1H), 5.49 (d, *J* = 16.5 Hz, 1H), 5.22 (br s, 1H), 4.42 – 4.28 (m, 2H), 4.23 – 4.12 (m, 2H), 3.10 (t, *J* = 6.8 Hz, 2H), 2.48 – 2.35 (m, 1H), 2.08 – 1.76 (m, 5H), 1.76 – 1.39 (m, 8H), 1.16 – 1.03 (m, 1H), 0.87 – 0.72 (m, 1H); ^{13}C NMR (101 MHz, MeOD/$CDCl_3$; 9:1) δ 175.7, 158.2, 158.1, 144.9, 144.7, 142.2 (x2), 132.5, 132.3, 128.5 (x2), 127.9 (x2), 126.0, 126.0, 120.7 (x2), 74.7, 67.7, 54.9, 48.1, 41.4, 41.1, 36.7, 36.6, 32.1, 30.1, 29.8, 24.9, 23.8; LC-MS (linear gradient 10 → 90% MeCN, 0.1% TFA, 11 min): R_t (min): 8.70 (ESI-MS (m/z): 521.13 ($M+H^+$)). Spectroscopic data was in agreement with literature.[18,23] The procedure was repeated on 2.0 mmol scale to obtain Fmoc-Lys(TCO)-OH (**17**, 942 mg, 1.81 mmol, 90%). The product was redissolved in dioxane and lyophilized to obtain a white powder for Fmoc SPPS.

*Note: no chemical shift differences were encountered on ^{1}H and ^{13}C NMR for the two diastereoisomers of compound **17**. The signals were therefore reported as a single compound.*

Ser(Trt)-Ile-Ile-Asn(MMt)-Phe-Glu(2-PhiPr)-Lys(TCO)-Leu-Tentagel S AC (20): Fmoc-Leu-Tentagel S AC resin (218 mg, 50 µmol, Rapp polymere) was swelled in DMF (2 mL; 30 min) and manually elongated using a repetitive cycle of: *i.* 20% piperidine in DMF (2 mL, 3 x 3 min; Fmoc deprotection); *ii.* DMF wash (4 x 2 mL); *iii.* Coupling (30 min; 60 min for **17**) with Fmoc-protected amino acid (250 µL, 1 M in DMF, 5 equiv), HCTU (250 µL, 1 M in DMF, 5 equiv) and DIPEA (500 µL, 1 M in DMF, 10 equiv); *iv.* DMF wash (4 x 2 mL); *v.* Ac_2O capping (5% *v/v* in DMF with 0.1 M DIPEA; 2 mL, 10 min); *vi.* DMF wash (4 x 2 mL). After Fmoc deprotection of the N-terminus, the resin was washed with DCM (3 x 2 mL) and Et_2O (3 x 2 mL) and subsequently dried over air to obtain **20** (254 mg) which was divided in portions for deprotection experiments.

Deprotection of 20 to obtain peptide fragments: Procedures were based on existing literature.[33] Ser(Trt)-Ile-Ile-Asn(MMt)-Phe-Glu(2-PhiPr)-Lys(TCO)-Leu-Tentagel S AC (**20**, 40 mg crude resin) was shaken in DCM (1 mL, 7 x 2 min). The resin was treated with a solution of TFA (5 / 10 / 20% *v/v*; 0.66 equiv) and TIS (2% *v/v*) in DCM (410 µL) for 1 hour before draining the reaction mixture in a 10 mL round-bottom flask containing MeOH (41 µL) and pyridine (64 / 128 / 258 µL; 2 equiv). The resin was washed with a solution of TFA (5 / 10 / 20% *v/v*; 0.33 equiv) and TIS (2% *v/v*) in DCM (200 µL). The neutralized mixture was stirred for 10 min, concentrated *in vacuo* and redissolved in MeCN/H_2O/*t*-BuOH (1:1:1, 100 µL). The resulting solution was sonicated (10 min), 10 x diluted with MeCN/H_2O/*t*-BuOH (1:1:1) and analyzed by LC-MS (20 µL injection). After the first measurement, tetrazine **21** (10 mM in DMSO, 10 µL) was added and the sample was analyzed once more by LC-MS (20 µL injection).

3.5 References

[1] J. Sauer, H. Wiest, *Angew. Chem.* **1962**, *74*, 353–353.

[2] E. M. Sletten, C. R. Bertozzi, *Angew. Chem. Int. Ed.* **2009**, *48*, 6974–6998.

[3] E. M. Sletten, C. R. Bertozzi, *Acc. Chem. Res.* **2011**, *44*, 666–676.

[4] J. A. Prescher, C. R. Bertozzi, *Nat. Chem. Biol.* **2005**, *1*, 13–21.

[5] B. L. Oliveira, Z. Guo, G. J. L. Bernardes, *Chem. Soc. Rev.* **2017**, *46*, 4895–4950.

[6] N. K. Devaraj, *ACS Cent. Sci.* **2018**, *4*, 952–959.

[7] M. L. Blackman, M. Royzen, J. M. Fox, *J. Am. Chem. Soc.* **2008**, *130*, 13518–13519.

[8] R. Selvaraj, J. M. Fox, *Curr. Opin. Chem. Biol.* **2013**, *17*, 753–760.

[9] M. T. Taylor, M. L. Blackman, O. Dmitrenko, J. M. Fox, *J. Am. Chem. Soc.* **2011**, *133*, 9646–9649.

[10] A. Darko, S. Wallace, O. Dmitrenko, M. M. Machovina, R. A. Mehl, J. W. Chin, J. M. Fox, *Chem. Sci.* **2014**, *5*, 3770–3776.

[11] N. K. Devaraj, R. Upadhyay, J. B. Haun, S. A. Hilderbrand, R. Weissleder, *Angew. Chem. Int. Ed.* **2009**, *48*, 7013–7016.

[12] N. K. Devaraj, S. Hilderbrand, R. Upadhyay, R. Mazitschek, R. Weissleder, *Angew. Chem. Int. Ed.* **2010**, *49*, 2869–2872.

[13] K. Lang, L. Davis, S. Wallace, M. Mahesh, D. J. Cox, M. L. Blackman, J. M. Fox, J. W. Chin, *J. Am. Chem. Soc.* **2012**, *134*, 10317–10320.

[14] T. Plass, S. Milles, C. Koehler, J. Szymański, R. Mueller, M. Wießler, C. Schultz, E. A. Lemke, *Angew. Chem. Int. Ed.* **2012**, *51*, 4166–4170.

[15] W. D. Lambert, S. L. Scinto, O. Dmitrenko, S. J. Boyd, R. Magboo, R. A. Mehl, J. W. Chin, J. M. Fox, S. Wallace, *Org. Biomol. Chem.* **2017**, *15*, 6640–6644.

[16] R. Rossin, S. M. Van Den Bosch, W. Ten Hoeve, M. Carvelli, R. M. Versteegen, J. Lub, M. S. Robillard, *Bioconjug. Chem.* **2013**, *24*, 1210–1217.

[17] Y. Fang, J. C. Judkins, S. J. Boyd, C. W. am Ende, K. Rohlfing, Z. Huang, Y. Xie, D. S. Johnson, J. M. Fox, *Tetrahedron* **2019**, *75*, 4307–4317.

[18] I. Nikić, T. Plass, O. Schraidt, J. Szymański, J. A. G. Briggs, C. Schultz, E. A. Lemke, *Angew. Chem. Int. Ed.* **2014**, *53*, 2245–2249.

[19] J.-E. Hoffmann, T. Plass, I. Nikić, I. V. Aramburu, C. Koehler, H. Gillandt, E. A. Lemke, C.

Schultz, *Chem. Eur. J.* **2015**, *21*, 12266–12270.

[20] R. M. Versteegen, R. Rossin, W. ten Hoeve, H. M. Janssen, M. S. Robillard, *Angew. Chem. Int. Ed.* **2013**, *52*, 14112–14116.

[21] R. Rossin, S. M. J. van Duijnhoven, W. ten Hoeve, H. M. Janssen, F. J. M. Hoeben, R. M. Versteegen, M. S. Robillard, *Bioconjug. Chem.* **2016**, *27*, 1697–1706.

[22] R. Rossin, R. M. Versteegen, J. Wu, A. Khasanov, H. J. Wessels, E. J. Steenbergen, W. ten Hoeve, H. M. Janssen, A. H. A. M. van Onzen, P. J. Hudson, M. S. Robillard, *Nat. Commun.* **2018**, *9*, 1484.

[23] J. Li, S. Jia, P. R. Chen, *Nat. Chem. Biol.* **2014**, *10*, 1003–1005.

[24] A. M. F. van der Gracht, M. A. R. de Geus, M. G. M. Camps, T. J. Ruckwardt, A. J. C. Sarris, J. Bremmers, E. Maurits, J. B. Pawlak, M. M. Posthoorn, K. M. Bonger, D. V. Filippov, H. S. Overkleeft, M. S. Robillard, F. Ossendorp, S. I. van Kasteren, *ACS Chem. Biol.* **2018**, *13*, 1569–1576.

[25] Y. Chiang, A. J. Kresge, *J. Am. Chem. Soc.* **1985**, *107*, 6363–6367.

[26] R. P. Kirchen, T. S. Sorensen, *J. Am. Chem. Soc.* **1979**, *101*, 3240–3243.

[27] J. E. Nordlander, K. D. Kotian, D. E. Raff, G. F. Njoroge, J. J. Winemiller, *J. Am. Chem. Soc.* **1984**, *106*, 1427–1432.

[28] M. S. Robillard, R. M. Versteegen, W. ten Hoeve, R. Rossin, *Chemically Cleavable Group*, **2014**, WO 2014/081303 A1.

[29] R. M. Versteegen, W. ten Hoeve, R. Rossin, M. A. R. de Geus, H. M. Janssen, M. S. Robillard, *Angew. Chem. Int. Ed.* **2018**, *57*, 10494–10499.

[30] T. Hori, K. B. Sharpless, *J. Org. Chem.* **1978**, *43*, 1689–1697.

[31] N. Becker, E. M. Carreira, *Org. Lett.* **2007**, *9*, 3857–3858.

[32] M. Royzen, G. P. A. Yap, J. M. Fox, *J. Am. Chem. Soc.* **2008**, *130*, 3760–3761.

[33] M. Mergler, *Synthesis of Fully Protected Peptide Fragments. In: Pennington M.W., Dunn B.M. (Eds) Peptide Synthesis Protocols. Methods in Molecular Biology, Vol 35*, Humana Press, **1994**.

[34] U. Neuenschwander, I. Hermans, *J. Org. Chem.* **2011**, *76*, 10236–10240.

[35] J. Farrera-Sinfreu, M. Royo, F. Albericio, *Tetrahedron Lett.* **2002**, *43*, 7813–7815.

[36] M. A. R. de Geus, G. J. M. Groenewold, E. Maurits, C. Araman, S. I. van Kasteren, *Chem. Sci.* **2020**, *11*, 10175–10179.

[37] E. Atherton, C. J. Logan, R. C. Sheppard, *J. Chem. Soc., Perkin Trans. 1* **1981**, 538–546.

[38] C.-D. Chang, M. Waki, M. Ahmad, J. Meienhofer, E. O. Lundell, J. D. Haug, *Int. J. Pept. Protein Res.* **2009**, *15*, 59–66.

[39] K. Barlos, D. Gatos, S. Koutsogianni, W. Schäfer, G. Stavropoulos, Y. Wenging, *Tetrahedron Lett.* **1991**, *32*, 471–474.

[40] C. Yue, J. Thierry, P. Potier, *Tetrahedron Lett.* **1993**, *34*, 323–326.

[41] P. Sieber, B. Riniker, *Tetrahedron Lett.* **1991**, *32*, 739–742.

[42] M. J. van de Graaff, T. Oosenbrug, M. H. S. Marqvorsen, C. R. Nascimento, M. A. R. de Geus, B. Manoury, M. E. Ressing, S. I. van Kasteren, *Bioconjug. Chem.* **2020**, *31*, 1685–1692.

[43] D. V. Kashelikar, C. Ressler, *J. Am. Chem. Soc.* **1964**, *86*, 2467–2473.

[44] S. Mojsov, A. R. Mitchell, R. B. Merrifield, *J. Org. Chem.* **1980**, *45*, 555–560.

[45] H. Gausepohl, M. Kraft, R. W. Frank, *Int. J. Pept. Protein Res.* **1989**, *34*, 287–294.

[46] R. F. Ribeiro, A. V. Marenich, C. J. Cramer, D. G. Truhlar, *J. Phys. Chem. B* **2011**, *115*, 14556–14562.

[47] T. Huhtiniemi, T. Suuronen, M. Lahtela-Kakkonen, T. Bruijn, S. Jääskeläinen, A. Poso, A. Salminen, J. Leppänen, E. Jarho, *Bioorg. Med. Chem.* **2010**, *18*, 5616–5625.